Thermal Evolution and Overpressurization of Europa's Subsurface Ocean

Austin Green

November 4, 2012

Advisor: Laurent Montesi

GEOL394H

1. Abstract

Scientific consensus on the mechanics of formation of ridge features on Europa has not yet been reached. Currently, the most popular model of ridge formation is the shear heating method, in which ridges develop as a result of strike-slip motion on a pre-existing crack. This strike-slip motion causes shear heating in the ice, leading to dilation of the ice that uplifts the flanks of the ridge and collapses the axial trough. However, There are other hypotheses of ridge formation that bear investigation. One possibility is that ridges are formed as the result of cryovolcanic processes acting between the outer ice shell and the subsurface ocean. Despite the higher density of liquid water when compared to ice, it is possible for cryovolcanism to occur if the ice shell exerts enough pressure on the ocean as a result of its gradual crystallization and expansion.

Studies on ocean pressurization have shown that the subsurface ocean is insufficiently pressurized to allow liquid water to penetrate through the entire ice shell and extrude on the surface. Therefore, the possibility of ridges forming as a result of extrusive processes is unlikely. Intrusive cryovolcanism may still be a mechanism for ridge formation if enough pressure exists to force water partially into the ice shell. As the water intrusion freezes, it will expand and buckle the surrounding shell.

A model of the thermal history and stress evolution of the liquid ocean and icy shell of Europa is constructed to determine if the ocean is pressurized enough to cause intrusive cryovolcanic activity. The final results from the thermal history model are used to estimate how the mass of the ice shell and the ocean change over time. This estimate will be used to calculate how much overpressure may be expected in the ocean and how far water may be forced into the ice shell as a result of this overpressure. The thermal evolution model shows that the ice shell on Europa crystallizes to a depth of 20 km in approximately 13 million years. This leads to 30 KPa of overpressure being exerted on the ocean. This overpressurization will lead to water intruding through approximately 91.2% of the total thickness of the ice shell, which may allow for sill formation in the upper depths of the shell.

2. Table of Contents

3. Introduction

Images returned by the *Galileo* spacecraft have revealed a variety of surface features on Europa. Jupiter's second Galilean Moon, Europa, exhibits more evidence of recent geologic activity than other bodies in our solar system many times its size, such as Mercury, Venus, and Mars. The cause of this geologic activity is Europa's orbital relationships with its fellow Galilean Satellites. Europa is locked in a 1:2:4 Laplace Resonance with its proximal and distal neighbors, Io and Ganymede, respectively, so that Europa's orbital period is twice that of Io's and half that of Ganymede's (Wiesel 1981). In this Laplace resonance, gravitational and tidal forces interacting amongst the satellites and Jupiter force the satellites into long-term orbital paths that would otherwise be unstable. Rather than gradually circularizing as most satellites do, all three satellites' orbital paths remain highly elliptical. This high orbital eccentricity causes massive tidal deformation and heat generation, driving the geologic activity on the surface and interior of these satellites (Peale 1979, Hussman and Spohn, 2004).

Europa possesses a differentiated internal structure (Anderson et al., 1998). Despite its icy surface, Europa is chiefly a rocky body, with a silicate mantle and a metallic core constituting most of its volume. Current estimates based on rough seismic data place the thickness of the entire water layer at approximately 120 km (Cammarano et al. 2006). The observation of an induced magnetic field near the surface (Khurana et al., 1998) confirmed that while the outermost surface of the satellite is solid ice, a major component of the H_2O layer is indeed a subsurface liquid ocean. Hussman and Spohn (2004) created a thermal evolution model of the ice shell incorporating tidal forces from orbital fluctuations in the resonances of Io and Ganymede. They determined with their model that, when starting from an all-liquid H_2O shell, the ocean will progressively crystallize through time, developing a thickness of approximately 20-25 km over 4.5 Ga in the present day (See Fig. 1).

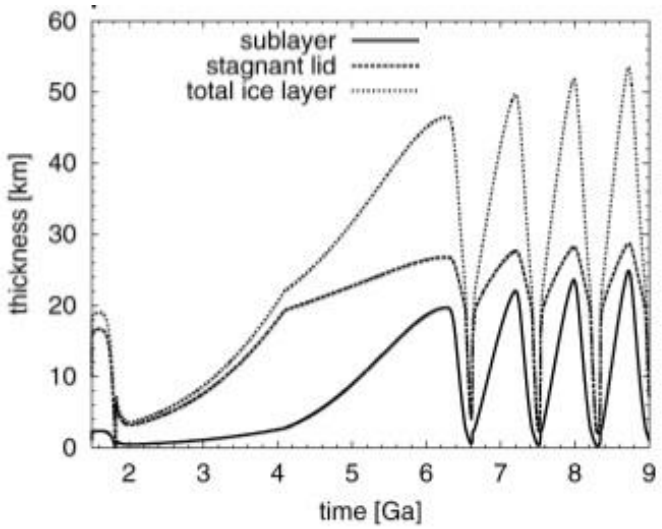

Fig. 1: Results of Hussmann and Spohn's study on the thermal evolution of Europa's ice shell. The model was run over 9 Gyrs, coupled with an orbital evolution model simulating the orbital relationships between Io and Ganymede. At the present day (4.5 Ga on this figure), the ice shell thickness is determined to be between 20 and 25 km thick.

The origin of the surface features of Europa classified as ridges, bands, chaos, and cyclods, is most likely strongly linked to its subsurface ocean. Researchers have devised many hypotheses about their formation since Galileo first observed Europa. The origin of ridges is particularly difficult to ascertain. Europan Ridges are long lineations on the surface of Europa characterized by two raised flanks surrounding a central axial trough (See Fig. 2). They are ubiquitous on Europa's surface and don't seem to have a clear analogue on other geologically active planetary bodies, such as Earth. The absence of similar ridges on rocky planets suggests that these features most likely are the result of interactions between a global ice shell and subsurface ocean; however, the specifics of these interactions are yet unclear.

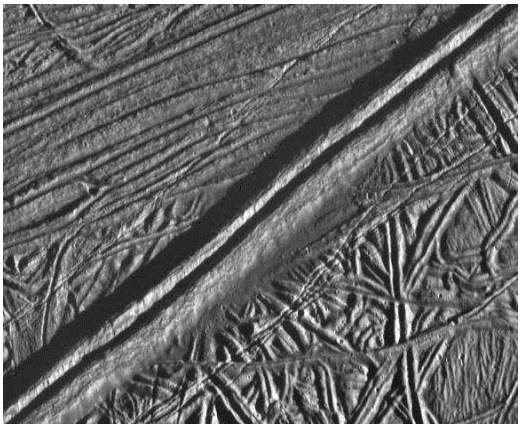

Fig. 2: A *Galileo* image of a ridge (Center). This picture clearly shows the major features of ridges: The raised flanks surrounding an axial trough. (Source: NASA-JPL)

Several hypotheses have been advanced in an effort to explain the surface ridges. Nimmo and Gaidos (2002) proposed that the ridges develop as a result of strike-slip motion on a pre-existing crack. This strike-slip motion would have caused shear

heating in the ice, leading to dilation of the ice along that uplifts the flanks of the ridge and collapses the axial trough. Fagents (2003) hypothesized that cryovolcanic water extrusions may explain the appearance of the ridges, along with many other Europan surface features. This project, however, addresses supporting evidence for the hypothesis first proposed by Melosh and Turtle (2004) and refined by Johnston and Montési (2012) that the ridges are influenced by cryovolcanic intrusions. In this model, liquid water fills a crack in the ice shell. However, instead of being extruded onto the surface, the water freezes as an intrusion. The expansion of the water as it freezes will force aside the surrounding ice, buckling it and reshaping it to cause uplift in the crack walls, forming the ridge morphology.

The cryovolcanic intrusion model requires that liquid water is able to fill cracks inside the ice shell. However, liquid water is more dense than ice, so it will not naturally rise through the ice shell. The hypothesis of this project is that overpressure on the liquid ocean is sufficient to inject water into cracks in the ice. As Europa cools over time, the internal ocean crystallizes progressively. The rigidity of the ice shell limits the expansion of the satellite that would be needed to accommodate this crystallization, causing the pressure of the internal ocean to increase instead. Manga and Wang (2007) have also investigated the mechanism of overpressure as a method for forcing water up the shell, and concluded that, at current estimates for the thickness of the ice shell, liquid water would not be under enough pressure to be extruded on the surface. This is a strong objection against the water extrusion hypothesis. However, Manga and Wang did not specify in their model whether the pressure was sufficient for water to simply penetrate the ice shell. It is necessary to evaluate how far into the crust pressurized water can penetrate to provide realistic impact to the cryovolcanic intrusion model of ridge formation.

4. Methods of Analysis

4.1 Model Description

4.1.1 Model Outline

The model is initially defined by a two-phase system in which an ice shell overlies a liquid ocean. This ice shell cools over time according to the heat conduction equation:

$$(1)\quad \frac{\partial T}{\partial t} = -\kappa \frac{\partial^2 T}{\partial z^2} + \kappa H_\varepsilon$$

T is temperature, t is time, z is depth from the surface, κ is diffusivity, and H_ε is heat produced by tidal flexure in the ice shell. As heat is lost at the bottom of the ice shell, the water will crystallize directly below the shell and thicken it over time by the following relation:

$$\frac{dz_m}{dt} = \frac{Q_m}{\rho L}\partial t \quad (2)$$

Q_m is the temperature gradient (dT/dz) at z_m, the depth of the base of the ice shell, L is the latent heat of fusion of ice, and ρ is the density of ice. The ice expands as it freezes, compressing the ocean and adding overpressure at a rate of $\delta P_{ex}/\delta z$. H_ε, dz_m/dt, and $\delta P_{ex}/\delta z$ are solved for numerically using the Runge-Kutta adaptive timestep differential equation solver built-in to MATLAB. The definition and value of all constant parameters is given in table 1.

In this model, the effects of spherical heat conduction are not considered, as the water layer of Europa is not a large enough fraction of its total radius for the spherical shape of the planet to have a major effect on heat transfer inside the shell. The shell may be considered a planar feature in terms of cooling with little effect on the final results.

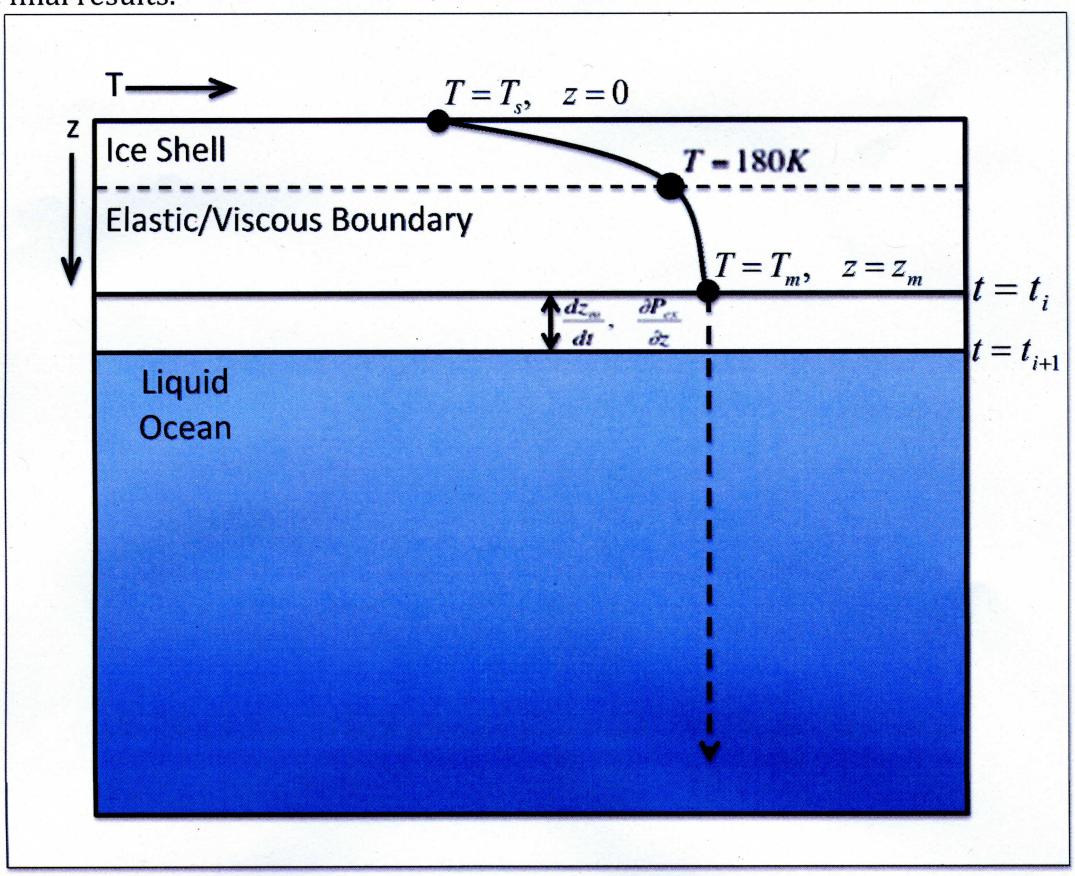

Figure 3: Schematic of model basics. The model is defined by a conductively cooling ice shell overlying a liquid ocean. The ice shell is defined by its upper boundary $T=T_s$ (110K), $z=0$ and its lower boundary $T=T_m$ (273K), $z=z_m$. The ice shell thickens over time at a rate of dz_m/dt and expands as water freezes at the bottom, increasing the excess pressure on the ocean at a rate of $\delta P_{ex}/\delta z$. P_{ex} is reduced on the ocean by radial displacement of the ice shell due to viscous deformation in the lower portion of the shell. The boundary line between the upper zone of elastic deformation, where P_{ex} is

evaluated, and the lower zone of viscous deformation is treated as the depth at which the ice temperature reaches 180K.

4.1.2 Heat Production by Tidal Flexure

Tidal flexure due to orbital interactions with Jupiter, Io, and Ganymede is the major source of heat production on Europa and is an essential factor of any thermal evolution model. Tidal heat production in an ice shell can be related to depth by means of the ice viscosity, η. The basic relation is as follows (After Tobie *et al.,* 2003):

$$H_s = \frac{2H_{Max}}{\left(\frac{\eta}{\eta_{Max}} + \frac{\eta_{Max}}{\eta}\right)} \quad (3)$$

Where ice viscosity is given by:

$$\eta = \eta_m \exp\left(-\gamma_t \frac{T - T_m}{\Delta T}\right) \quad (4)$$

With η_m being the viscosity at ice's melting point, and γ_t being a material constant. H_{max} and η_{max} are determined by:

$$H_{Max} = \frac{\mu\varepsilon^2}{\omega} \quad (5)$$

$$\eta_{Max} = \frac{\mu}{\omega} \quad (6)$$

With μ being the bulk shear modulus, ω being the orbital frequency, and ε being the average tidal strain rate experienced by Europa. By using the temperature profiles determined by the thermal evolution model described below, these equations provide an assessment of the tidal heat dissipation at any depth in the ice shell. This heat production counteracts conductive cooling over time and can bring the ice shell's thickness to a steady state.

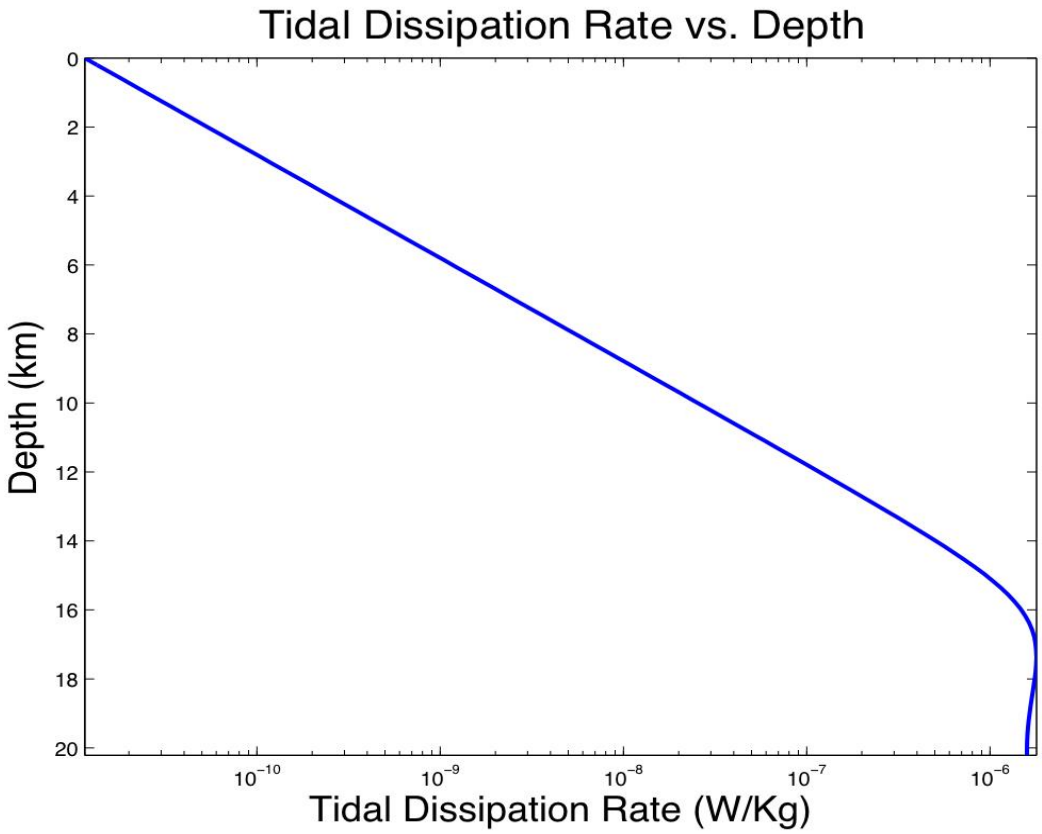

Figure 4: Sample tidal dissipation profile generated by applying the equations above to an ice shell of 20 km thickness with a standard half-space cooling geotherm.

4.1.3 Thermal Evolution Model: The Stefan Problem

In the absence of the heating processes described above, the thermal evolution model is described as a Stefan Problem: the simultaneous cooling and solidification of a liquid. As a special case of the half-space cooling model in which a moving phase boundary is present, the analytical solution to the Stefan Problem is well known. It is given by:

(7)

Where η and λ are defined as:

$$\eta = \frac{z}{\sqrt{\kappa t}} \quad (8)$$

$$\frac{L\sqrt{\pi}}{C_p(T_m - T_s)} = \frac{e^{-\lambda^2}}{\lambda \operatorname{erf}(\lambda)} \quad (9)$$

As this analytical solution does not accommodate any heat production, The Stefan Problem must be solved numerically in this model so that tidal dissipation may be added. The numerical solution will be addressed further in section 5.2.2. This analytical model is still useful, however, in calibrating any numerical model of the Stefan Problem. If heat production is temporarily discounted in the numerical model, it can be directly compared to this well-known analytical solution, determining if the numerical solution is sound.

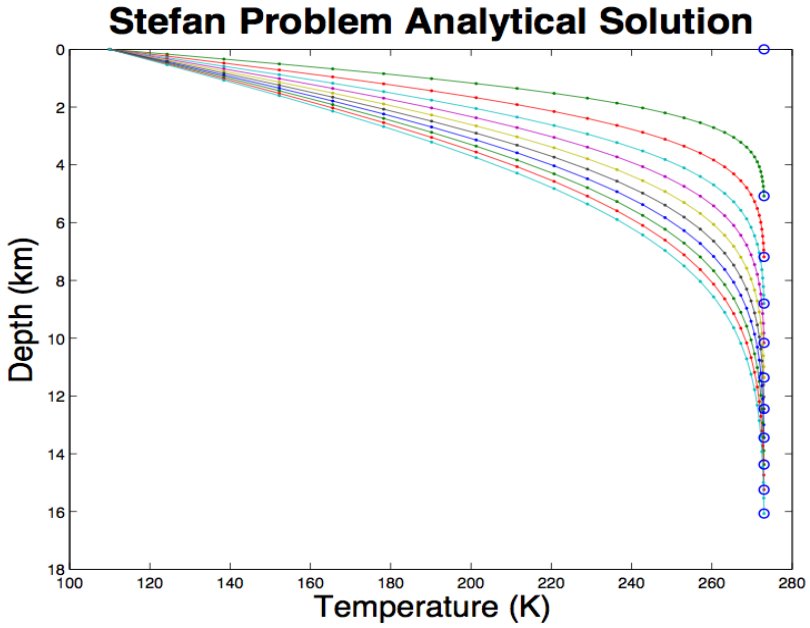

Figure 5: Analytical solution of the Stefan Problem for an ice shell. This profile can be used to verify the accuracy of the numerical model developed to accommodate for heat production.

4.1.4 Stress Evolution

Using ice thickness results from the thermal evolution stage of the model, the increase in over pressure with depth $\delta P_{ex}/\delta z$ can be determined. This stage of the model treats the water layer as two concentric spherical shells on a Europa-sized body with radius R. The basic equation to determine this overpressurization is as follows (After Manga and Wang, 2007):

$$(10)\quad \frac{\partial P_{ex}}{\partial z_m} = \frac{3(\rho_w - \rho_i) r_i^3}{\beta \rho_w (r_i^3 - r_c^3)}$$

Where β is the compressibility of water, ρ_w and ρ_i are the densities of water and ice, respectively, r_i is the inner radius of the ice shell, and r_c is the inner radius of the entire water layer. However, the lower portion of this ice shell will deform viscously, causing an upward radial displacement u_r and reducing the overall excess pressure. In this model, the radius ξ at which the transition between elastic and viscous deformation occurs in the ice shell is taken at the depth the temperature in the ice shell reaches 180K. The radial displacement experienced by such an ice shell is:

$$(11)\quad u_r = -\frac{\xi}{E}(\sigma_r - 2\upsilon\sigma_t)$$

Where E is the Young's Modulus, ν is the Possion ratio, σ_r is the radial stress of the shell, and σ_t is the tangential stress of the shell. The solutions for the radial and tangential stresses in the shell are as follows:

$$(12)\quad \sigma_r = \frac{P_{ex}(z_m)}{\left(\frac{R}{\xi}\right)^3 - 1}\left[1 - \left(\frac{R}{\xi}\right)^3\right]$$

$$(13)\quad \sigma_t = \frac{P_{ex}(z_m)}{\left(\frac{R}{\xi}\right)^3 - 1}\left[1 + \frac{1}{2}\left(\frac{R}{\xi}\right)^3\right]$$

This radial displacement and shell expansion will then decrease the overpressure by:

$$(14)\quad \delta P = \frac{3u_r r_i^2}{\beta(r_i^3 - r_c^3)}$$

Equations 10-14 are solved numerically in order to determine the total amount of excess pressure built up by the ice shell crystallized by the thermal evolution model. Manga and Wang (2007) found that for ice thicknesses greater than 1 km, σ_t exceeds the tensile strength of ice by a factor large enough for cracks to form at the base of the shell and propagate up the entire width of the shell to the surface. At this point, water will rise through the crack to the point of neutral buoyancy, which is determined in relation to overpressurization in equation 15.

$$(15)\quad H = \left(\frac{\rho_w - \rho_i}{\rho_w}\right)(R - r_i) - \frac{P_{ex}}{\rho_w g}$$

If $H \leq 0$, water is sufficiently pressurized to extrude onto the surface. Equation 15 can be then solved for P_{crit}, the amount of overpressure necessary for water to extrude on the surface.

Parameter	Value	Definition
T_s	110K	Surface temperature
T_m	273K	Melting temperature of ice
C_p	2050 kJ*K/kg	Specific heat capacity of ice
L	334 kJ/kg	Latent heat of fusion of water
R	1569000 m	Planetary radius
g	1.315 m/s^2	Acceleration due to gravity
r_c	1449000 m	Radius to base of water layer
β	4x10^{-10} Pa^{-1}	Compressibility of water
E	5x10^9	Young's modulus
v	0.33	Poisson's ratio
ρ_i	910 kg/m^3	Density of ice
ρ_w	1000 kg/m^3	Density of water
ε	10^{-10} s^{-1}	Tidal strain rate
ω	2x10^{-5} s^{-1}	Orbital frequency
μ	3.3x10^9 Pa	Shear modulus
γ_t	0.0807	Dimensionless material constant
η_m	10^{14} Pa*s	Viscosity of ice at melting point

Table 1: Definition of model parameters.

4.2 Numerical Implementation

4.2.1 Calibration of The Thermal Evolution Solver

In a steady state ($\partial T/\partial t = 0$), subjected to the boundary conditions that temperature is fixed at T_s, the average surface temperature of Europa (110 K), at z=0, and T_m, the melting temperature of ice (273 K), at z=h, the bottom of the ice shell, the conductive heat flow equation admits the following solution:

$$T = T_s + \left(\frac{T_m - T_s}{h} + \frac{\alpha h}{2\kappa}\right)z - \frac{\alpha}{2\kappa}z^2 \quad (16)$$

After obtaining a steady state temperature profile from this equation, the finite difference method is used to numerically calculate Q, the temperature gradient (K/m). The numerical equation used to find Q is as follows:

$$Q = \frac{T_i - T_{i-1}}{z_i - z_{i-1}} \quad (17)$$

In order to evaluate the error associated with the model, another finite difference calculation is conducted of Q vs. z in order to come up with a numerical approximation of α, termed H:

$$H = \kappa \frac{Q_j - Q_{j-1}}{z_j - z_{j-1}} \quad (18)$$

The error of the model is given by the difference between H and α:

$$E = \frac{H - \alpha}{\alpha} \quad (19)$$

To further test the accuracy of the finite differences, consider that α varies linearly with depth. The steady state temperature solution becomes:

$$T = T_s + \left(\frac{T_m - T_s}{h} + \frac{3\alpha_0 h + \beta h^2}{6\kappa} \right) z - \frac{\alpha_0}{2\kappa} z^2 - \frac{\beta}{6\kappa} z^3 \quad , \quad \alpha = \alpha_0 + \beta z \quad (20)$$

The same error analysis as before was conducted on this solution.

The next model calibration step is to add and calibrate time-dependence. First a discrete time-dependent temperature model is constructed using the Euler method of numerically solving Ordinary Differential Equations. The Euler Method is the simplest ODE solver, but it tends to be unstable. In order to implement the Euler method, a simple temperature profile is first constructed as the initial conditions in which the surface value is T_s and every depth interval thereafter is equivalent to T_m. Then, H is numerically solved for at each depth (Eq. 6) and multiplied by a time interval dt. This Hdt value is then added to each corresponding value in the T matrix, along with α. This process is repeated in time step intervals of dt until a maximum time t_{max} is reached.

In order to make sure this time-dependent temperature solver functions properly, the relative error is evaluated by comparing the T values at thermal equilibrium state to the steady state model using a relative error calculation similar to Eq. 19.

After evaluating the error when compared to the steady-state model, it is then compared to an analytical solution of the half-space cooling model, derived from a solution of Eq. 1:

$$T = T_s - (T_m - T_s) erf\left(\frac{y}{\sqrt{\kappa t}}\right) \quad (21)$$

This error analysis will determine whether the intermittent time steps are also accurate when compared to analytical solutions.

4.2.2 Crystallization of the Ice Shell

The Stefan Problem in the presence of internal heating does not have a straightforward numerical solution. The standard numerical method of utilizing a time-independent static grid that evaluates temperature at regularly spaced depth nodes proved to be ineffective. The major obstacle provided by modeling the Stefan Problem is tracking the movement of z_m. This movement between time steps is determined numerically by applying the finite difference numerical method to equation (2), producing:

$$\frac{dz_m}{dt} = \frac{\left(\frac{T_{z_m} - T_{z_{m-1}}}{z_m - z_{m-1}}\right)}{\rho L} \partial t \quad (22)$$

Modeling the movement of z_m on a static numerical grid becomes problematic, however, as the value of z_m would generally fall between depth nodes at which the temperature is evaluated. Attempting to accommodate for this irregularity while also preserving the static grid caused the numerical model to become highly unstable and inaccurate, necessitating the implementation of a new numerical procedure. Instead of using a static, time-independent numerical grid, a moving time-dependent numerical grid is applied. This numerical procedure is outlined in figure 6.

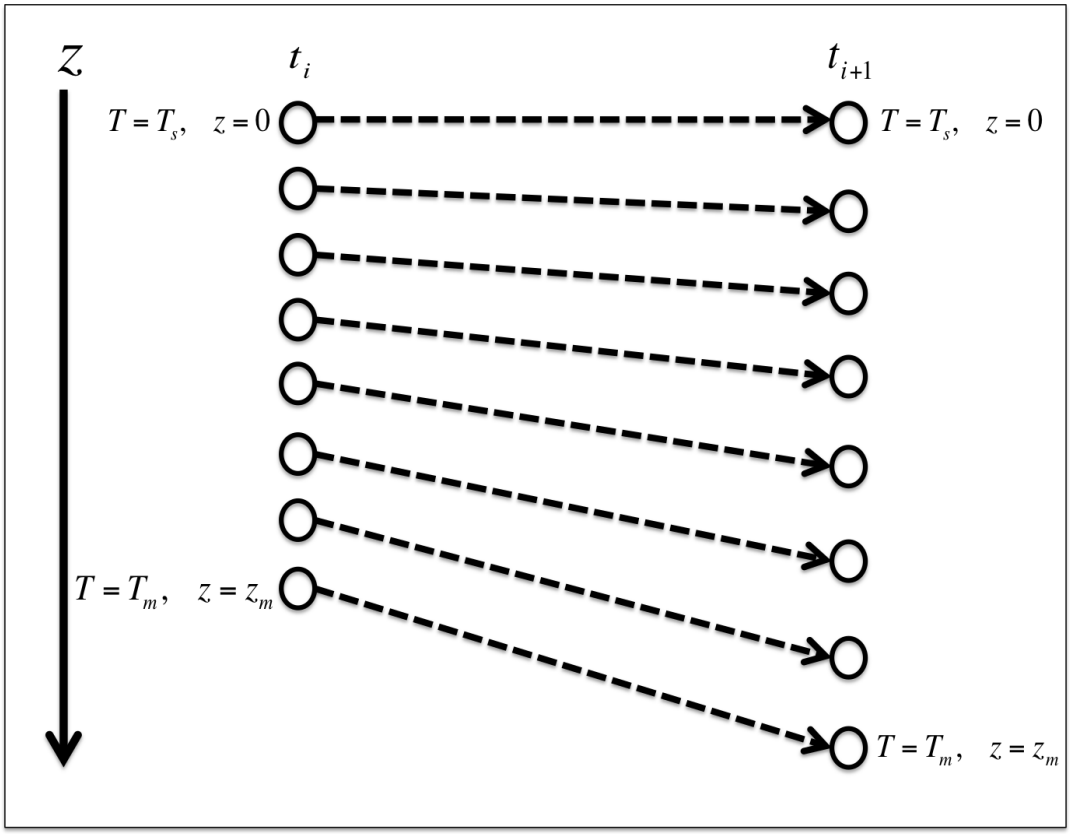

Figure 6: Moving coordinate procedure. At time step t_i, a depth profile with boundaries at z=0 and z=z_m is defined. The temperature gradient is computed by finite difference and dz_m/dt is determined from Q_m at z=z_m. dz_m/dt is then added to z_m to produce z_m at time t_{i+1}. The depth of each node is updated at the next time step t_{i+1} to form a regular grid between the surface and the value of z_m.

Defining the lower boundary of the numerical grid at z_m for every time step allows for much greater flexibility and ensures that the location of the freezing front, as the most crucial result of the thermal evolution model, is always at the focal point of the model. In order to adapt the heat conduction equation (1) to this numerical procedure and accurately evaluate the temperature of the ice shell, an additional term must be added to the heat conduction equation to accurately scale the temperature profile with each renewed depth profile. The numerical relation that defines the change in temperature over time then becomes:

$$\frac{dT_i}{dt} = \kappa \frac{Q_{i+1} - Q_{i-1}}{z_{i+1} - z_{i-1}} + \left(\frac{T_i - T_{i-1}}{z_i - z_{i-1}} \right) \frac{T_m - T_{m-1}}{(z_m - z_{m-1})\rho L} + \kappa H_\varepsilon \quad (23)$$

Where H_ε is the tidal heat experienced in the shell, determined according to the solutions of equations (3-6) when applied to the temperature conditions given by the model. This procedure is run through MATLAB's native ODE solver, ODE45.

4.2.3 Stress Evolution Model

Due to an amount of circularity inherent in the solving for P_{ex}, σ_r, and σ_t (equations 10, 12, and 13) equations 10-14 must be combined into one numerical relation to accurately calculate overpressure. The combined equation then becomes:

$$(24) \quad P_{ex}\left\{\frac{\beta(r_i^3-r_c^3)}{3r_i^2}-\frac{\xi}{E\left(\frac{R}{\xi}\right)^3-1}\left[1-2\upsilon-(1+\upsilon)\left(\frac{R}{\xi}\right)^3\right]\right\}=\frac{\rho_w-\rho_i}{\rho_w}\delta z_m$$

The stress evolution model is then coupled with the thermal evolution model and uses temperature results to determine viscoelastic deformation boundary depth ξ, as well as z_m values returned by the model to determine r_i at every time step.

5. Presentation of Results and Discussion

5.1 Calibration

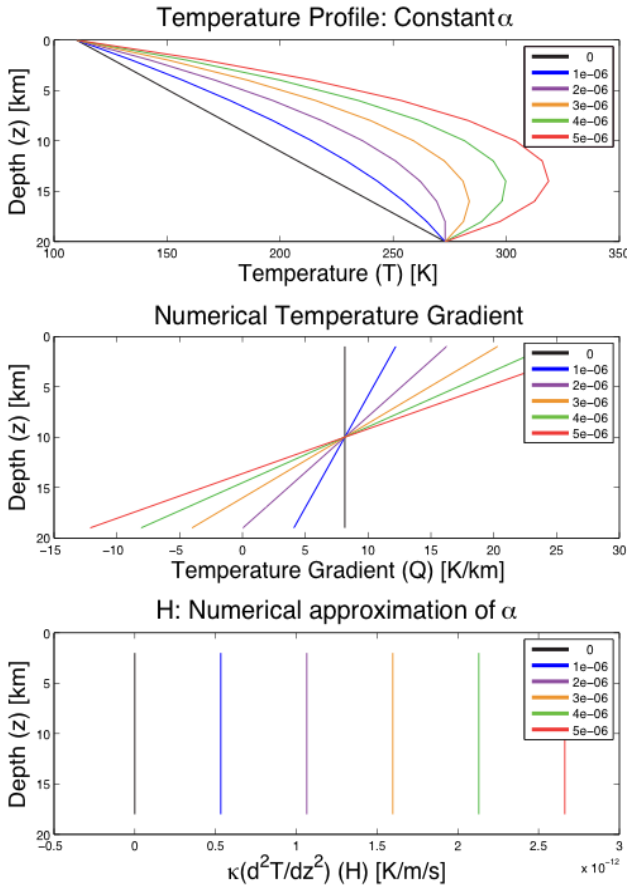

Figure 7: Thermal profile for the first steady-state solution with constant α. **Top:** Temperature vs. Depth steady state profile for several values of α according to Eq. 2. **Middle:** Numerically defined

temperature gradient derived from the Temperature/Depth profile above according to Eq. 3.
Bottom: Numerically defined Heat value according to Eq. 4.

Figure 7 shows the results of the very first model, the steady state temperature profile with constant α, used to evaluate the accuracy of the Finite Difference approximation. These charts are modeled off of equations 2, 3, and 4, respectively. The value of h in this case is taken to be 20 km. One may note that, in the temperature profile itself, T extends significantly past the melting point of ice, 273 K. While this is a physical impossibility, the goal is to calibrate the accuracy of my model, rather than simulate reality. After producing these charts, Eq. 5 is then applied to the results of H. The error figure is pictured in figure 8.

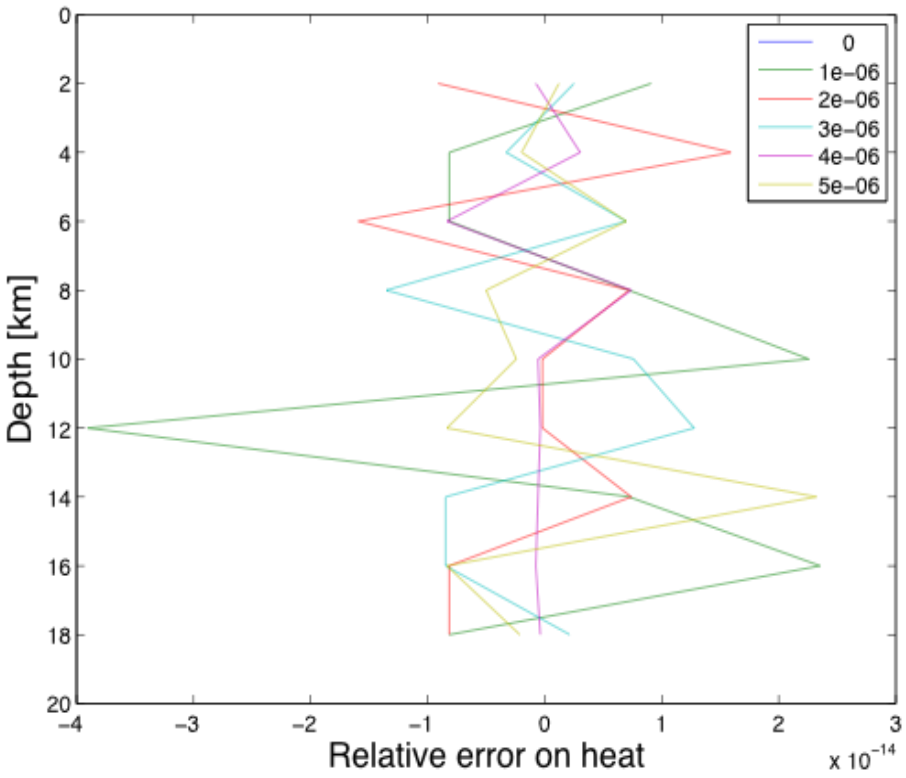

Figure 8: Relative error on numerical H value according to Eq. 5.

As the error results are registered on the order of 10^{-14}, this first iteration of the model can be considered very accurate. The next step is to model this same procedure but with Eq. 6, the steady state profile with a linear αrather than Eq. 2.

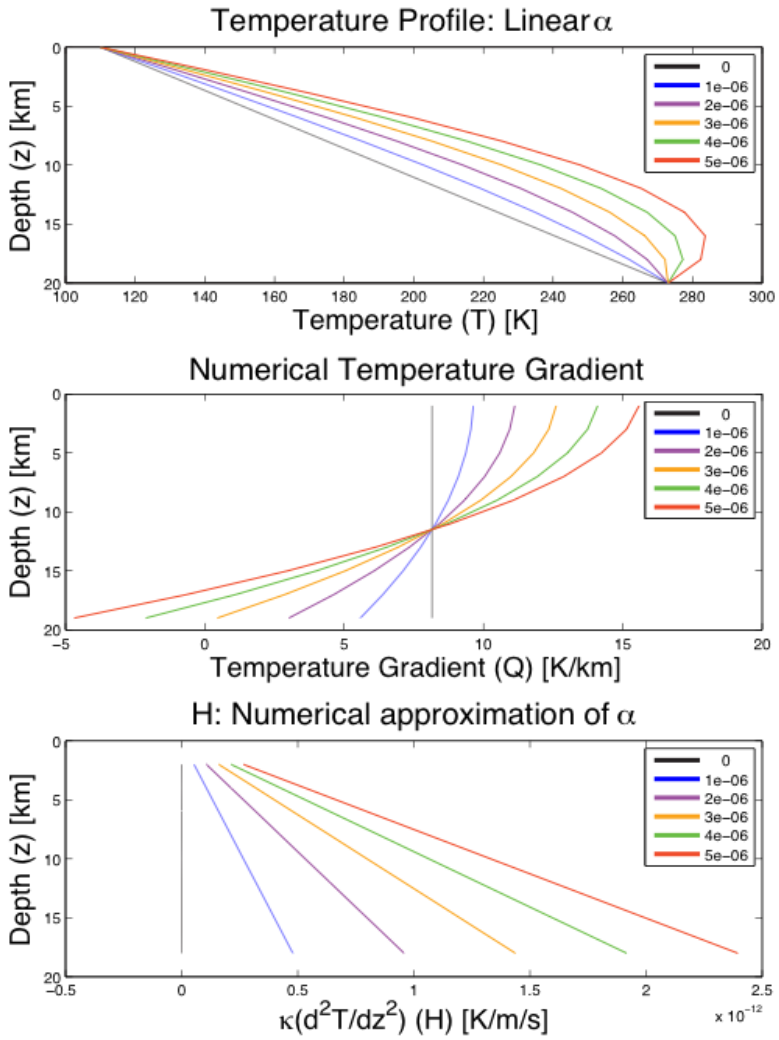

Figure 9: Thermal profile for the first steady-state solution with constant α. **Top:** Temperature vs. Depth steady state profile for several values of α according to Eq. 6. **Middle:** Numerically defined temperature gradient derived from the Temperature/Depth profile above according to Eq. 3. **Bottom:** Numerically defined Heat value according to Eq. 4. Legend in all three figures refer to the value of α.

The major effect of having a linear α value is that the temperature profile no longer extends quite so far past T_m. Otherwise these results are very similar to the first model. The error measurements for this second model are shown in figure 10.

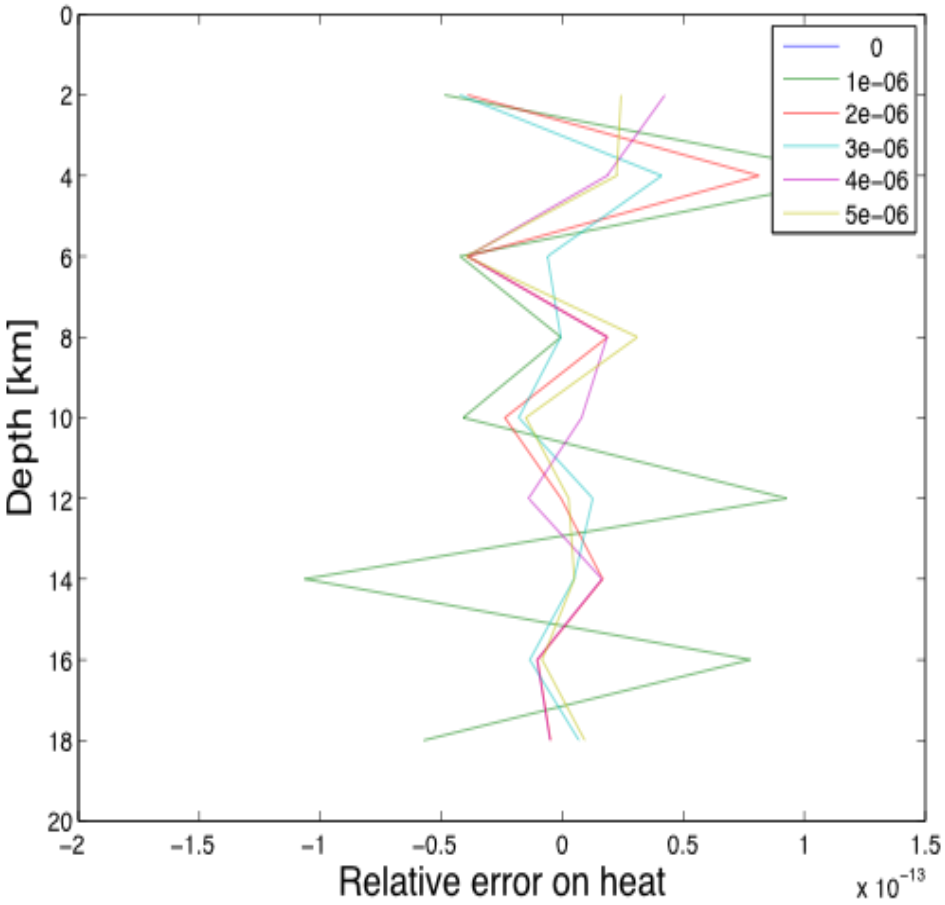

Figure 10: Relative error on *H* value for the second profile.

Although the relative error is an order of magnitude higher for this iteration of the model, it is still negligible, which indicates that the model is still accurate. Next the results of the test of the time-dependent Euler model are presented (Figure 11), as compared at its thermal equilibrium state to the steady-state model.

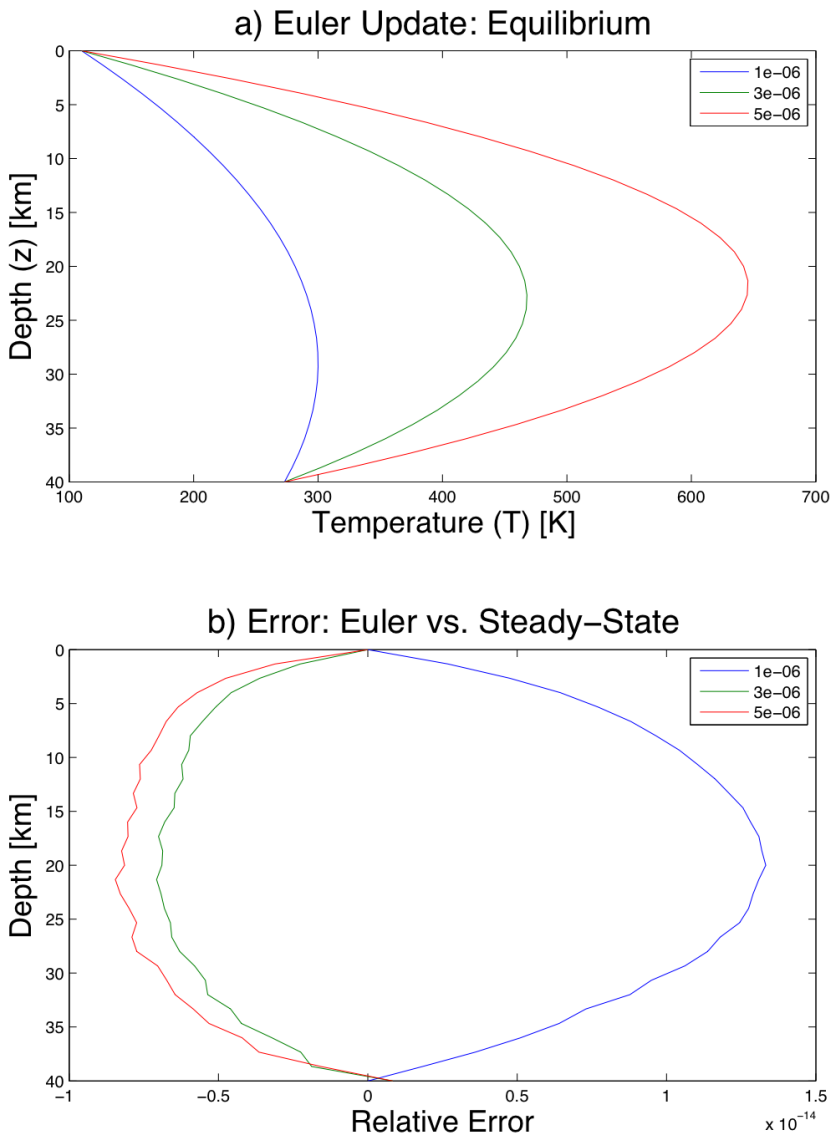

Figure 11: a) The thermal equilibrium state profile for the Euler Update method with h defined as 40 km. Three values of α are applied. **b)** The relative error returned from comparing the thermal equilibrium state to the steady-state analytical model.

The end state of the Euler update model also is shown to be highly accurate for several values of α, with relative error figures on the order of 10^{-14} when compared to the steady-state model. However, the weakness of the Euler update in the intermediate time steps is shown by its comparison with the half-space cooling model (Figure 12).

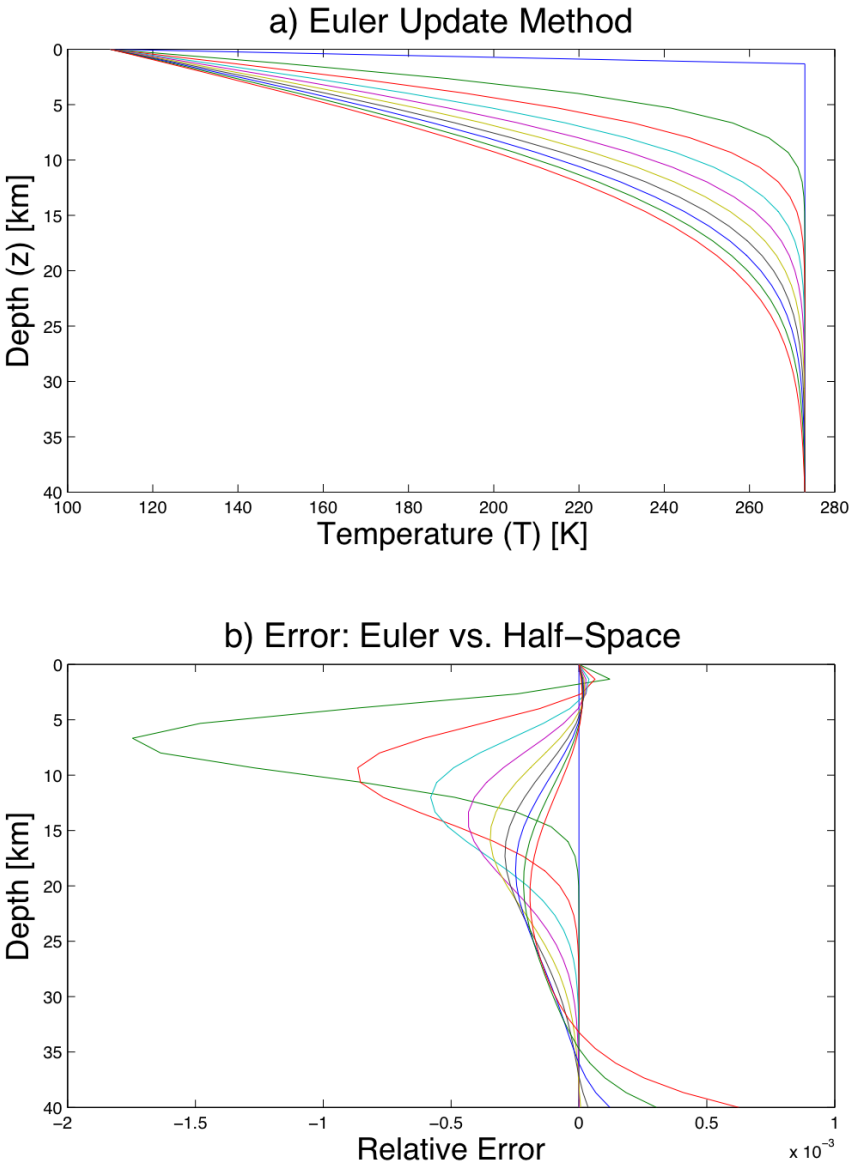

Figure 12: a) Full time-dependent temperature/depth profile using the Euler update method. Several time steps are shown in different colors. **b)** Relative error evaluated by comparing the Euler method to the half-space cooling analytical model (Eq. 21).

There are several prominent features of this error diagram. The most dramatic is the spike in relative error between 5 and 10 kilometers depth. This error spike is due to weaknesses in the Euler method as an ODE solver. The other interesting error feature is the "tail" feature at the bottom of the error profile. This is due to the fact that, unlike the Euler method, the half-space cooling model has no set depth limit. The half-space model, therefore, extends its cooling beyond the limit of the Euler model and it is difficult to match the very bottom of the temperature profile to the Euler method. These error numbers are the largest yet, on the order of magnitude of 10^{-3}, but this can be attributed to the Euler method's weaknesses as a discrete method.

The final calibration step compares the analytical solution of the Stefan problem with the numerically obtained crystallization calculation. In order to compare the two solutions, the heat production term in the numerical model is removed. A comparison of the movement of the freezing front over time for both models is shown in figure 13.

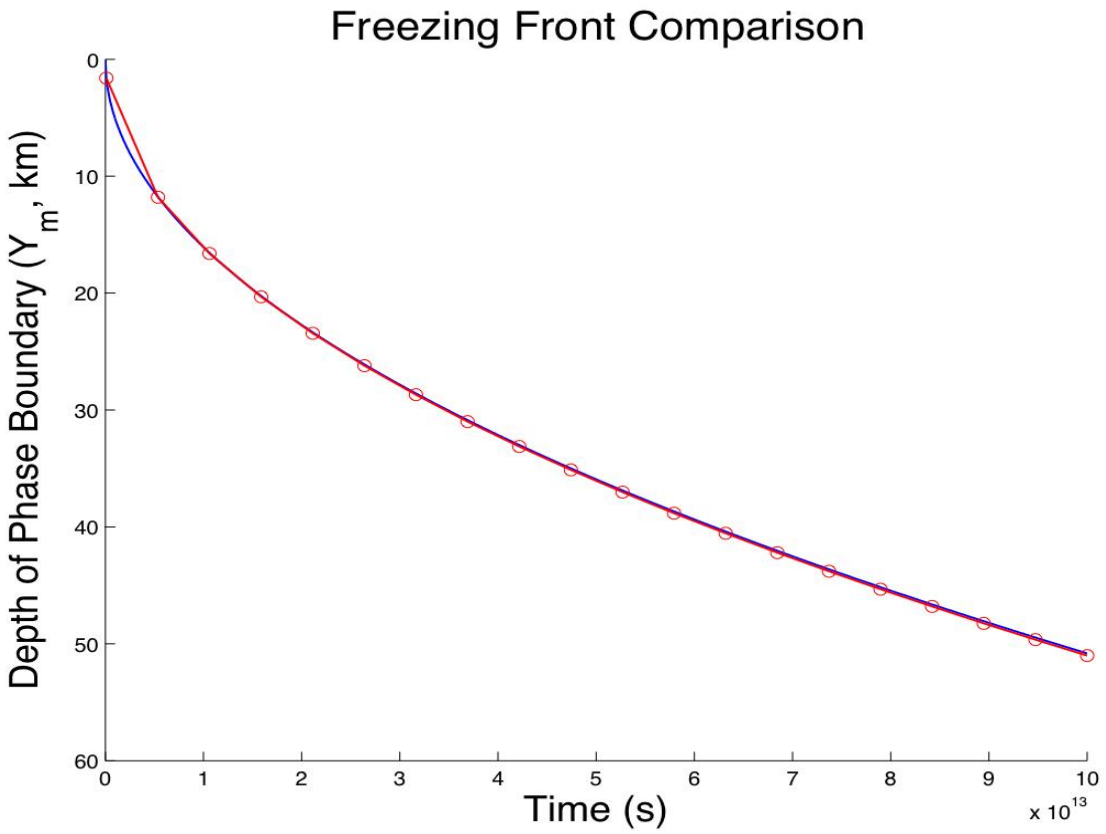

Figure 13: Comparison of freezing front depth calculated analytically (in blue) and the results of the numerical model (in red) without heat generation.

This result shows that the numerical moving grid procedure is stable enough to accurately reproduce the output of the well-known analytical solution. This numerical procedure is the foundation of every other component in the model, as the temperature profile data and the ice thickness data produced by this procedure are used to determine both tidal heat generation and overpressurization.

5.2 Thermal Evolution Model

When applied to Europa, the thermal evolution model indicates that the ice shell would reach a steady-state thickness of approximately 20 km in approximately 13

million years. These results are shown in Figure 14 as a mass estimate of the ocean and the ice shell.

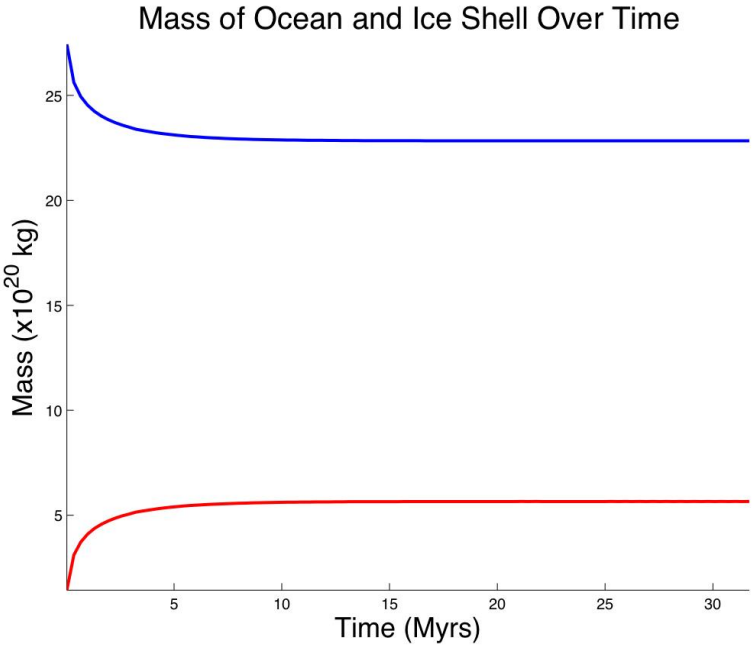

Figure 14: Time evolution of the mass estimate of the ocean (In blue) and the ice shell (In red). Ice thickness was converted into mass assuming that the ice shell corresponds to the upper layer of a 100-km thick water/ice spherical shell on a body of Europa's radius.

If the initialization of crystallization is taken at the time of Europa's formation, 4.5 Ga, this result makes overpressure an unlikely cause of recently formed surface features on Europa, as viscous flow at the base of the ice shell would probably have dissipated the pressure generated early on in the satellite's history. However, if Europa has undergone orbital evolution at any point in its history, the change in orbital parameters may allow the ice shell to melt and restart the crystallization and pressurization process. In order to investigate this, the thermal evolution model was run several times under varying orbital parameters (Figure 15).

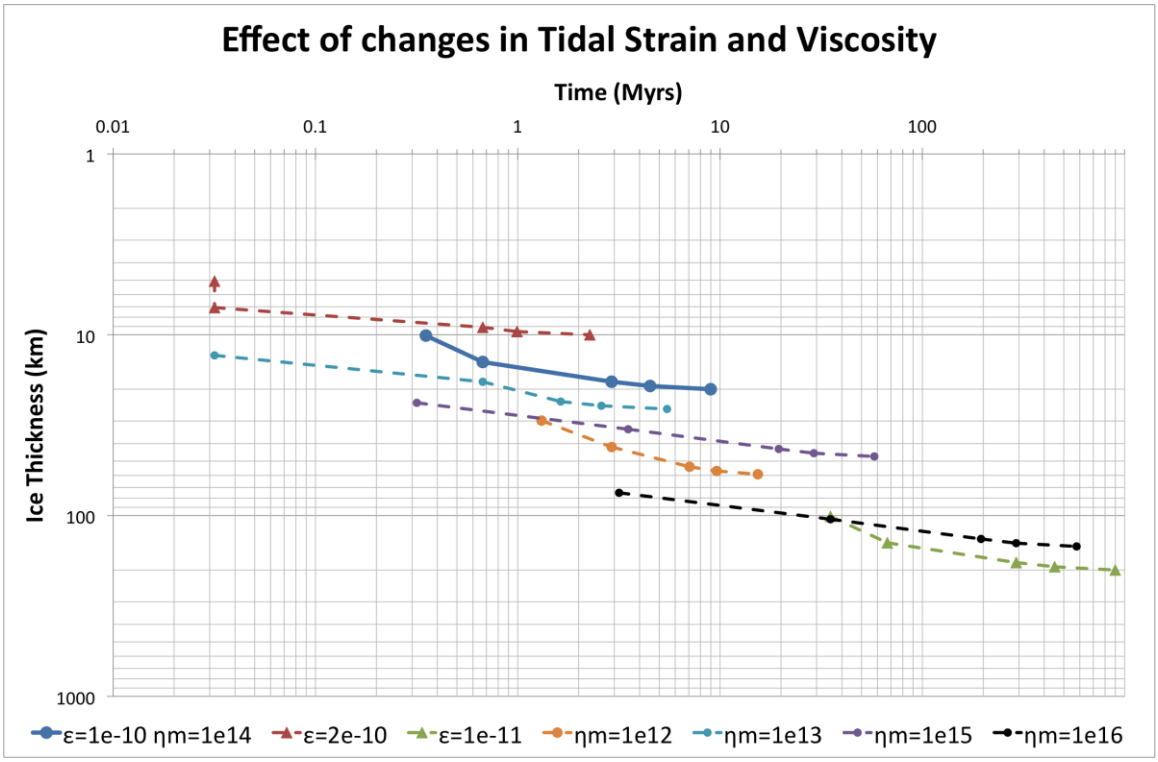

Figure 15: Time needed for the ice to reach a certain thickness. Each marker represents ice at 50%, 70%, 90%, 95%, and 99% of the maximum thickness. The solid line represents the conditions found on Europa $\varepsilon=10^{-10}$ s^{-1}, $\eta_m = 10^{14}$ Pa s . The series marked with triangles assume different tidal strain, and the series marked with circles assume a different ice viscosity.

As is seen in Figure 13, changing the tidal strain rate can have dramatic effects on the final thickness of the ice shell and the time it takes for the shell to crystallize. Increasing the strain rate by a factor of 2 crystallizes a shell that is half as thick in a small fraction of the time. On the other hand, decreasing the strain rate by an order of magnitude would crystallize the entire water layer of Europa. The effects of ice viscosity on the final thickness of the shell are less clear. No matter if you increase or decrease the viscosity, the shell crystallizes slower and thicker than with conditions found on Europa. This is a curious finding of the model. The true viscosity of Europa's ice is not well constrained, and if it differs from terrestrial ice, it would have large implications for both the thickness of the ice shell at thermal equilibrium and the time necessary to crystallize it. These trials also explain the difference between this model and the results found by Hussmann and Spohn (2004) shown in Figure 1. The model by Hussman and Spohn is coupled with a full orbital evolution model, allowing the thickness of the ice to adjust with changing orbital parameters. This model is only able to evaluate ice crystallization at the current orbital parameters.

If an orbital fluctuation, or an interaction with one of Europa's sister satellites such as Ganymede or Io were to increase Europa's eccentricity and therefore tidal strain rate, it would throw the ice shell out of thermal equilibrium and large-scale melting will result. If the tidal strain were to subsequently relax, the shell would begin

crystallizing again and building up pressure. Most estimates place the age of Europa's surface at approximately 90 Ma, which suggests that such an orbital fluctuation may have occurred in the last 100 million years. A buildup of overpressure over the 13 million years the ice shell crystallizes according to this model is a more plausible mechanism to create the surface features visible today if the ice shell started crystallizing at 90 Ma.

5.3 Stress Evolution Model

Figure 16 presents the values of P_{ex} over time for ice shell conditions matching the results of the thermal evolution model shown in figure 13.

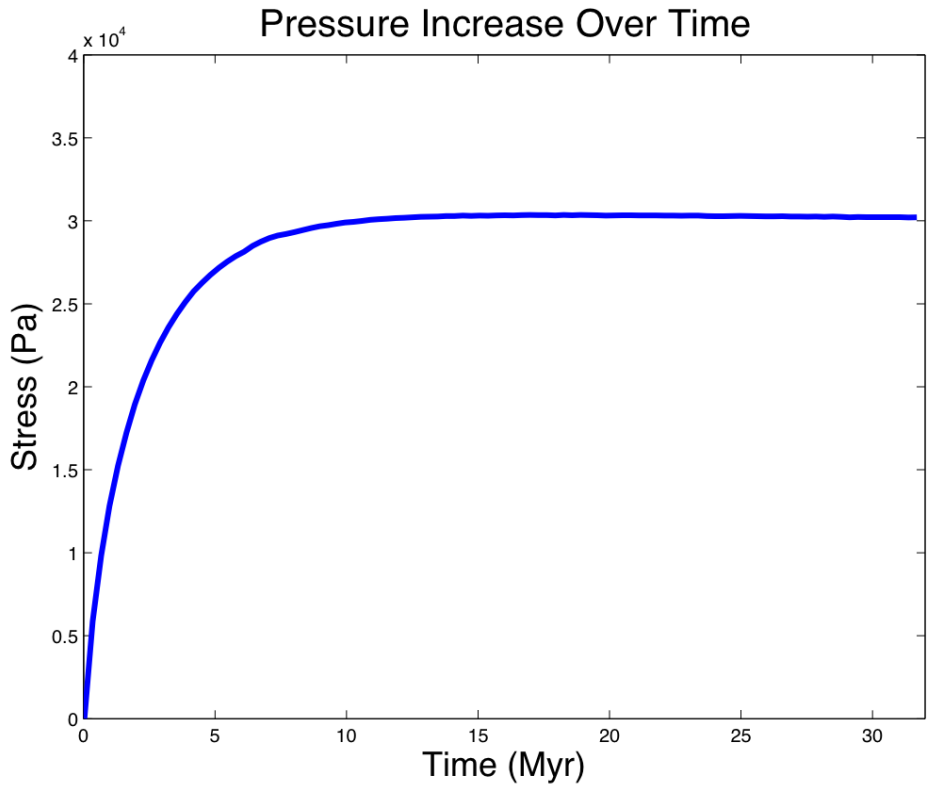

Figure 16: Excess pressure buildup over time result according to coupled Thermal/Stress evolution model.

These results indicate that the maximum excess pressure experienced by the ocean under the conditions of this model is approximately 30 kPa. Compared to equivalent ice shell thicknesses run through a similar model by Manga and Wang (2007), this model indicates a slightly lower buildup of excess pressure. This is most likely due to the addition in this model of a thermal evolution component, allowing for a much more specific cutoff point for elastic deformation than the assumption in Manga and Wang's study that the temperature of the ice reaches 180K at 1/3 of its total thickness. When the thermal evolution model is discounted and the static cutoff

used by Manga and Wang is instated in this model, the results match those reported by Manga and Wang closely. Manga and Wang (2007) found that water was not able to erupt onto the surface of Europa by pressure alone, but the possibility may still exist that partial intrusion into the ice shell occurs. A comparison of the results of this model with a calculation of P_{crit} over time also shows that extrusion is impossible by overpressure alone (Figure 16).

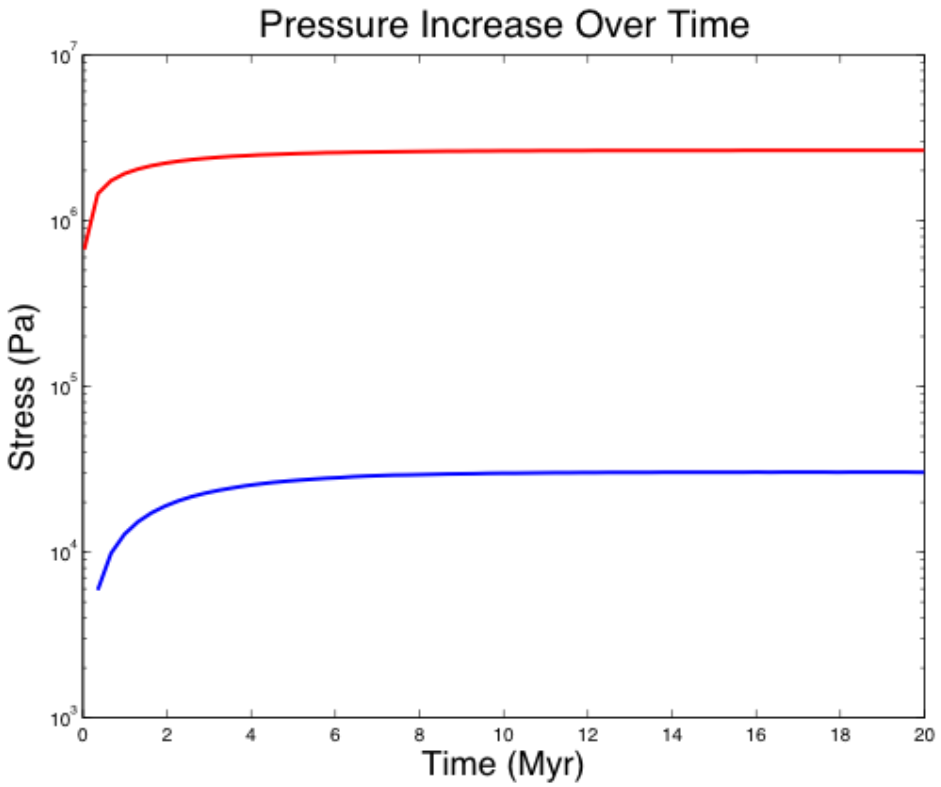

Figure 17: Comparison of results of stress evolution P_{ex} (In blue) with the amount of overpressure P_{crit} necessary for water extrusion (In red).

Water will still rise some distance through the ice shell, even though there is not enough pressure to extrude water on the surface. Using equation 15 and the ice shell thickness returned by the thermal evolution model, a view of the penetration depth achieved by water on Europa can be established. (Figure 17)

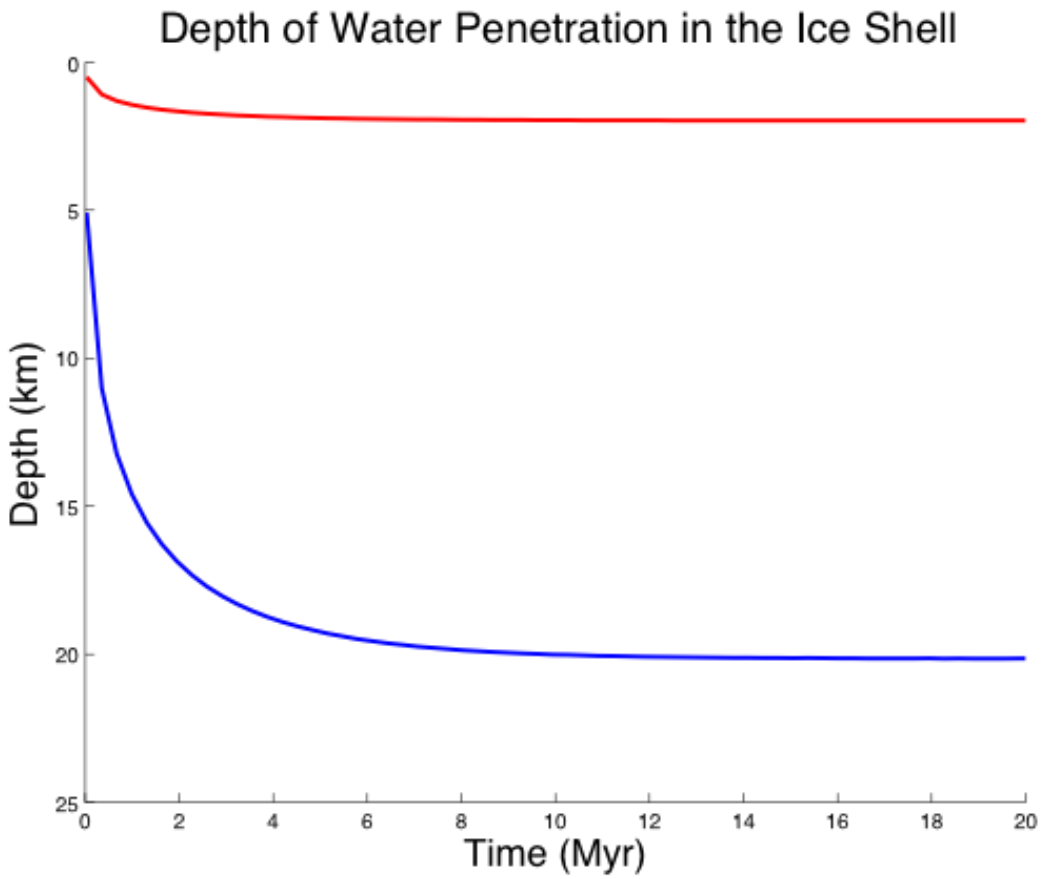

Figure 18: Final result: Depth profile of ice shell over time with the surface of Europa being set to 0 km. The blue line represents the base of the ice shell, and the red line represents the maximum depth above the base to which water will rise.

6. Conclusions and Future Work

Figure 17 shows that, depending on the thickness of the ice shell, water will rise to a level anywhere from ~.5 to ~1.8 km beneath the surface. As both the difference in density between water and ice and overpressurization play a role in this, it is important to determine each factor's relative contribution to this rise in water. The most direct way to evaluate this is to present the result as a relative proportion of the total thickness of the ice shell rather than as a depth beneath the surface. If treated this way, the depth to which water will rise increases from 91.0% of the ice shell's total thickness to 91.2% of the ice shell's total thickness over a period of 15 Ma. As the initial value of overpressure is treated as zero, it can be concluded that overpressure contributes to 0.2% of the relative rise through the ice shell. Overall, overpressure seems to play a very small role in Europan cryovolcanism. One other interesting result of the model is that the maximum water level decreases over time, rather than increasing as may be expected. Because H is also determined by relative

density and the current thickness of the ice layer, these results do make sense if overpressure is not a large contributor to water rise. The fact that water can be found in more shallow depths earlier during the crystallization process may be useful for future modeling. The absolute data will also be useful in modeling cryovolcanic sills, which may be a major cause of present surface features.

There are still some properties about the ocean of Europa that are still not well constrained. This may allow pressurization to be a larger factor. It is well-known that there are ions in solution in Europa's ocean, as the satellite has a generated magnetic field. The presence of these ions may change the properties of both the ocean and the ice shell in many ways. These ions may raise or lower the melting temperature of the ice, which will affect the natural thickness of the ice shell. Additionally, these ions will serve to increase the bulk density of the water. An increase in water density, however, will correspond to a decrease in water penetration. The neutral buoyancy point will decrease as water becomes proportionally more dense than ice.

Another uncertain factor in this model is the true thickness of the water/ice layer. If the water layer of Europa was thinner but the ice shell remained the same thickness, overpressurization may increase over time. After having done some preliminary hypothetical calculations looking into this possibility, it seems that the relative thickness of the water and ice layers actually plays a negligible role in overpressurization. Referring to equation 24, the reason for this seems to be that the compressibility of water, β, is so small, at 4×10^{-10} Pa^{-1}, it completely negates any effect the relative sizes of the water and ice layers may have. This result is a little counterintuitive, but it makes sense when one scrutinizes the math.

Another aspect to be considered would be a more detailed approach to tidal heating in the shell. Tobie et al. has done further work on their tidal dissipation models that have not been considered in this model, which will further refine these results and help determine a more accurate time frame for reaching steady state. There are also alternative models of tidal heating that can be incorporated into this model. The most popular tidal stress model besides the diurnal model that this paper uses is tidal stresses generated by the non-synchronous rotation of the ice shell. This non-synchronous rotation causes a periodic cycle of increasing and decreasing tidal strain on a regional scale as the relative location of the planetary tidal strain axis changes with respect to the decoupled shell. This will cause the shell to locally melt and recrystallize on a semi-regular basis as tidal strain increases and decreases.

The major flaw in this model is that the possibility of a convecting layer in the ice shell is not considered. Many other thermal evolution models (e.g. Showman and Han 2003, Tobie et al. 2003, Hussmann and Spohn 2004) indicate that a convecting layer in the lower portion of the ice shell is an important component. This model does not consider it mainly due to time constraints, but the addition of a convective layer in the ice may have large implications on my final result and may change it drastically.

In summary, overpressurization seems to have less of an impact on Europan cryovolcanism and Europan surface geology as was once thought. Other mechanisms of transporting water up the shell should be searched for. Although water does rise through a significant portion of the ice shell according to this model, that rise is chiefly accounted for by the relative densities of water and ice. There are several parameters considered in this model that are still uncertain on Europa, and these may impact overpressurization and water intrusion, but it seems that the effect would be either negligible or negative. Despite all this, these results ultimately indicate that cryovolcanic sills are still a possibility that merits future investigation.

7. Bibliography

Anderson, J.D., G. Schubert, R. A. Jacobson, E. L. Lau, W. B. Moore, and W. L. Sjogren 1998. Europa's differentiated internal structure: Inferences from four Galileo encounters. *Science* **281**, 2019-2022.

Cammarano, F., Lekic, V., Manga, M., Panning, M. and Romanowicz, B. (2006). Long period seismology on Europa: 1. Physically consistent interior models. *Journal of Geophysical Research* **111.** *doi: 10.1029/2006JE002710. issn: 0148-0227.*

Fagents, S.A. 2003. Considerations for effusive cryovolcanism on Europa: The post-Galileo perspective. *Journal of Geophysical Research* **108**.

Gaeman, J., S. Hier-Majumder, and J.H. Roberts 2012. Sustainability of a subsurface ocean within Triton's interior. *Icarus* **220**, 339-347.

Hussmann, H., and T. Spohn 2002. Thermal Equilibrium States of Europa's Ice Shell: Implications for Internal Ocean Thickness and Surface Heat Flow. *Icarus* **156,** 143-151.

Hussmann, H., and T. Spohn 2004. Thermal-orbital evolution of Io and Europa. *Icarus* **171**, 391–410

Khurana, K. K, M. G. Kivelson, D. J. Stevenson, G. Schubert, C. T. Russell, R. J. Walker, and C. Polanskey 1998. Induced magnetic fields as evidence for subsurface oceans in Europa and Callisto. *Nature* **395**, 777–780.

Manga, M., and C.-Y. Wang 2007. Pressurized oceans and the eruption of liquid water on Europa and Enceladus. *Geophysical Research Letters* **34**.

Melosh, H.J., and E.P. Turtle 2004. Ridges on Europa: Origin by Incremental Ice Wedging. *Lunar and Planetary Science* **35**.

Nimmo, F., and E. Gaidos 2002. Strike-slip motion and double ridge formation on Europa. *Journal of Geophysical Research* **107**.

Ojakangas, G. W., and D. J. Stevenson 1989. Thermal state of an ice shell on Europa. *Icarus* **81**, 220–241.

Peale, S.J., P. Cassen, and R.T. Reynolds 1979. Melting of Io by Tidal Dissipation. *Science* **203**, 892-894.

Showman, A.P., and L. Han. Numerical simulations of convection in Europa's ice shell: Implications for surface features. *Journal of Geophysical Research* **109**.

Sohl, F., T. Spohn, D. Breuer, and K. Nagel 2002. Implications from Galileo observations on the interior structure and chemistry of the Galilean satellites. *Icarus* **157**, 104-119.

Tobie, G., Choblet, G., and Sotin, C. 2003. Tidally heated convection: constraints on Europa's ice shell thickness. *Journal of Geophysical Research **108.*** doi:10.1029/2003JE002099

Wiesel, W. 1981. The origin and evolution of the great resonance in the Jovian satellite system. *Astronomical Journal* **86**, 611-618.